Supplementary Information

Quantification of the Mixed-Valence and Intervalence Charge Transfer Properties of a Cofacial Metal-Organic Framework *via* Single Crystal Electronic Absorption Spectroscopy

Patrick W. Doheny,[a] Jack K. Clegg,[b] Floriana Tuna,[c] David Collison,[c] Cameron J. Kepert*[a] and Deanna M. D'Alessandro*[a]

[a] School of Chemistry, The University of Sydney, New South Wales, 2006, Australia.

[b] School of Chemistry and Molecular Biosciences, The University of Queensland, St. Lucia, Queensland, 4072, Australia.

[c] Department of Chemistry and Photon Science Institute, The University of Manchester, Manchester M13 9PL, United Kingdom.

* Corresponding authors' phone: +61 2 93513777; email: deanna.dalessandro@sydney.edu.au; cameron.kepert@sydney.edu.au

Synthesis

4-(4-Formylphenyl)pyridine. 4-(4-Formylphenyl)pyridine was prepared according to a literature procedure.[1] 4-Bromobenzaldehyde (2.00 g, 10.8 mmol), 4-pyridylboronic acid (1.59 g, 12.9 mmol), potassium carbonate (7.46 g, 54.0 mmol) and $Pd(PPh_3)_4$ (0.30 g, 0.26 mmol, 2.4 mol%) were suspended in a degassed solution of 1,4-dioxane (75 mL) and water (7.5 mL) and refluxed under N_2 overnight. The mixture was allowed to cool to room temperature at which point water (30 mL) was added to yield a precipitate that was extracted three times with dichloromethane (3 × 60 mL). The organic layers were combined and dried over $Mg(SO_4)$ before the solvent was removed *in vacuo*. The crude residue was then purified by column chromatography (hexane : EtOAc : Et_3N 1:1:0.05) to yield the product as colourless needles (1.30 g, 7.10 mmol, 69%). ^{1}H NMR ($CDCl_3$, 300 MHz): δ 10.09 (s, 1H), 8.73 (d, $^3J_{H\text{-}H}$ = 4 Hz, 2H), 8.02 (d, $^3J_{H\text{-}H}$ = 8.2 Hz, 2H), 7.81 (d, $^3J_{H\text{-}H}$ = 8.2 Hz, 2H), 7.56 (d, $^3J_{H\text{-}H}$ = 4 Hz, 2H) ppm.

2,5-Bis(4-(pyridin-4-yl)phenyl)thiazolo[5,4-*d*]thiazole (BPPTzTz). Dithiooxamide (0.13 g, 1.08 mmol) and 4-(4-formylphenyl)pyridine (0.27 g, 1.47 mmol) were dissolved in DMF (2 mL) and heated at reflux overnight to give a dark suspension. After cooling to room

temperature, the mixture was cooled in ice and filtered to obtain the crude product that was then washed with water. Recrystallisation of the crude product from DMF gave the pure ligand as a brown powder (112 mg, 0.25 mmol, 22%). ^{1}H NMR (*d*-TFA, 300 MHz): δ 8.85 (d, $^{3}J_{\text{H-H}}$ = 5.6 Hz, 4H), 8.37 (d, $^{3}J_{\text{H-H}}$ = 5.5 Hz, 4H), 8.28 (d, $^{3}J_{\text{H-H}}$ = 7.8 Hz, 4H), 8.09 (d, $^{3}J_{\text{H-H}}$ = 7.9 Hz, 4H) ppm. ^{13}C{^{1}H} NMR (*d*-TFA, 75 MHz): δ 174.9, 160.8, 150.5, 143.6, 140.2, 136.1, 131.4, 130.6, 127.1 ppm. ESI-MS (ESI^{+}, MeCN): *m*/*z* calculated for $C_{26}H_{16}N_4S_2$ $[M + H]^{+}$ = 449.09; Found = 449.03 (100%). Elemental Analysis: Found: C 68.98%, H 3.59%, N 12.38%, S 14.02%; Calculated for $C_{26}H_{16}N_4S_2$: C 69.62%, H 3.60%, N 12.49%, S 14.29%.

Additional Crystallographic Details

Crystallography of BPPTzTz. A single colourless block crystal of the BPPTzTz ligand was mounted using a thin film of Paratone *N* oil on a diffractometer employing a Dectris EIGER X 16M detector and Silicon Double Crystal monochromated synchrotron radiation in a stream of nitrogen gas at 100(2) K at the MX2 beamline of the Australian synchrotron.[2] The structure was solved by intrinsic phasing in the triclinic *P*-1 (#2) space group using the SHELXT[3] program with further refinements and computations carried out using SHELXL-2018/3[4] within the ShelXle graphical user interface.[5] The structure was treated as a two-component pseudo-merohedral twin using the TwinRotMat package within the PLATON[6] program with the BASF parameter refining to 0.457. The non-hydrogen atoms in the asymmetric unit were modelled with anisotropic displacement parameters and a riding model with group displacement parameters for the hydrogen atoms. An empirical absorption correction was applied to the data using the SADABS code.[7]

The asymmetric unit (Figure S1 (a)) consisted of a two crystallographically distinct BPPTzTz ligands, the backbone of which (Figure S1 (b)) were found to be effectively planar.

Additional Instrumental Details

Thermal Gravimetric Analysis (TGA). TGA analysis was performed using a TA Instruments Discovery Thermogravimetric Analyser from 25-600 °C at 2 °C min^{-1} under a flow of nitrogen gas (0.1 L min^{-1}).

Crystallographic Tables

Table S1. Crystallographic data and refinement details for **CdTzTz**.

Formula	$C_{38}H_{32}N_6O_6S_3Cd$
Molecular weight / g mol^{-1}	877.27
Temperature / K	100(2)
Crystal system	orthorhombic
Space group	*Pcca*
a / Å	19.0673(3)
b / Å	26.1197(6)
c / Å	15.5005(3)
α / °	90
β / °	90
γ / °	90
Volume / Å^3	7719.7(3)
Z	8
ρ_{calc} / g cm^{-3}	1.510
μ / mm^{-1}	0.782
F(000)	3568.0
Crystal size / mm^3	0.183 × 0.164 × 0.016
Radiation	MoKα (λ = 0.71073 Å)
2Θ range for data collection / °	4.548 to 50.054
Index ranges	$-22 \le h \le 22$, $-31 \le k \le 31$, $-18 \le l \le 18$
Reflections collected	92102
Independent reflections	6828 [R_{int} = 0.0528, R_{sigma} = 0.0200]
Data / restraints / parameters	6828 / 706 / 659
Goodness-of-fit on F^2	1.079
Final R indexes [$I \ge 2\sigma(I)$]	R_1 = 0.0804, wR_2 = 0.2123

* $R_1 = \Sigma||F_o| - |F_c||/\Sigma|F_o|$ for $F_o > 2\sigma(F_o)$; $wR_2 = (\Sigma w(F_o^2 - F_c^2)^2/\Sigma(wF_c^2)^2)^{1/2}$ all reflections $w=1/[\sigma^2(F_o^2)+(0.0896P)^2+13.3135P]$ where $P=(F_o^2+2F_c^2)/3$

Table S2. Crystallographic data and refinement details for BPPTzTz.

Formula	$C_{26}H_{16}N_4S_2$
Molecular weight / g mol^{-1}	448.55
Temperature / K	100(2)
Crystal system	triclinic
Space group	*P*-1
a / Å	5.6650(11)
b / Å	7.5500(15)
c / Å	22.845(5)
α / °	80.52(3)
β / °	86.53(3)
γ / °	88.94(3)
Volume / Å^3	962.0(3)
Z	2
ρ_{calc} / g cm^{-3}	1.549
μ / mm^{-1}	0.302
F(000)	464.0
Crystal size / mm^3	0.120 × 0.070 × 0.015
Radiation	Synchrotron (λ = 0.71073 Å)
2Θ range for data collection / °	1.81 to 50.052
Index ranges	$-6 \leq h \leq 6$, $-8 \leq k \leq 8$, $-21 \leq l \leq 27$
Reflections collected	3039
Independent reflections	3039 [R_{sigma} = 0.0779]†
Data / restraints / parameters	3039 / 0 / 290
Goodness-of-fit on F^2	1.013
Final R indexes [$I \geq 2\sigma(I)$]	R_1 = 0.0600, wR_2 = 0.1545

* $R_1 = \Sigma||F_o| - |F_c||/\Sigma|F_o|$ for $F_o > 2\sigma(F_o)$; $wR_2 = (\Sigma w(F_o^2 - F_c^2)^2/\Sigma(wF_c^2)^2)^{1/2}$ all reflections $w=1/[\sigma^2(F_o^2) + (0.0896P)^2 + 13.3135P]$ where $P=(F_o^2 + 2F_c^2)/3$

† Structure was refined as a pseudo-merohedral twin, as such an R_{int} value is not reported.

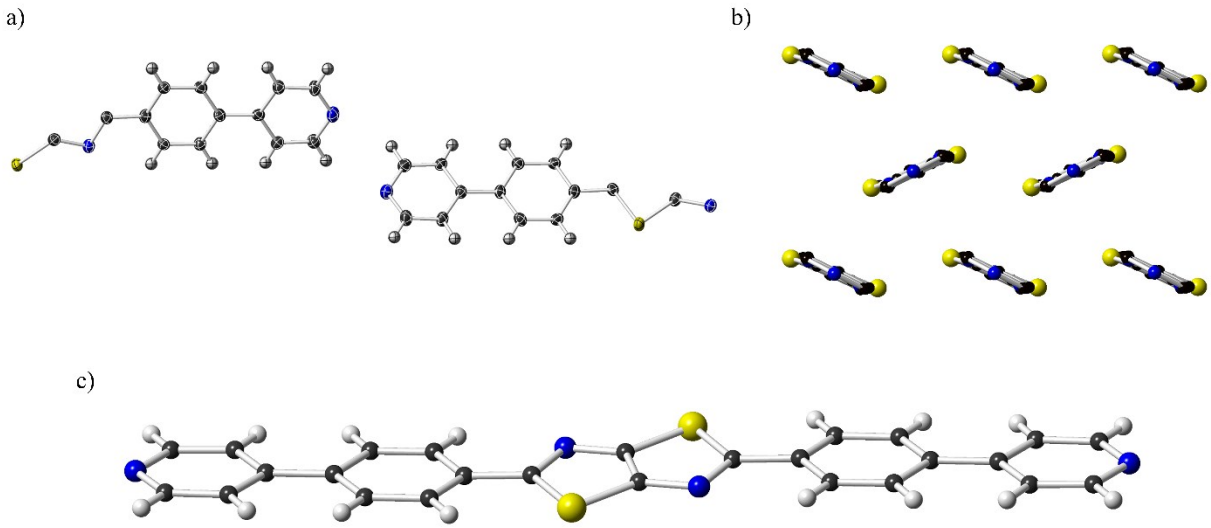

Figure S1. Crystal structure of the BPPTzTz ligand showing a) the asymmetric unit with thermal ellipsoids at 50% probability and b) crystal structure viewed down the *c*-axis and c) the planar backbone of the ligand. Atom labelling: S = yellow, N = blue, C = grey and H = white.

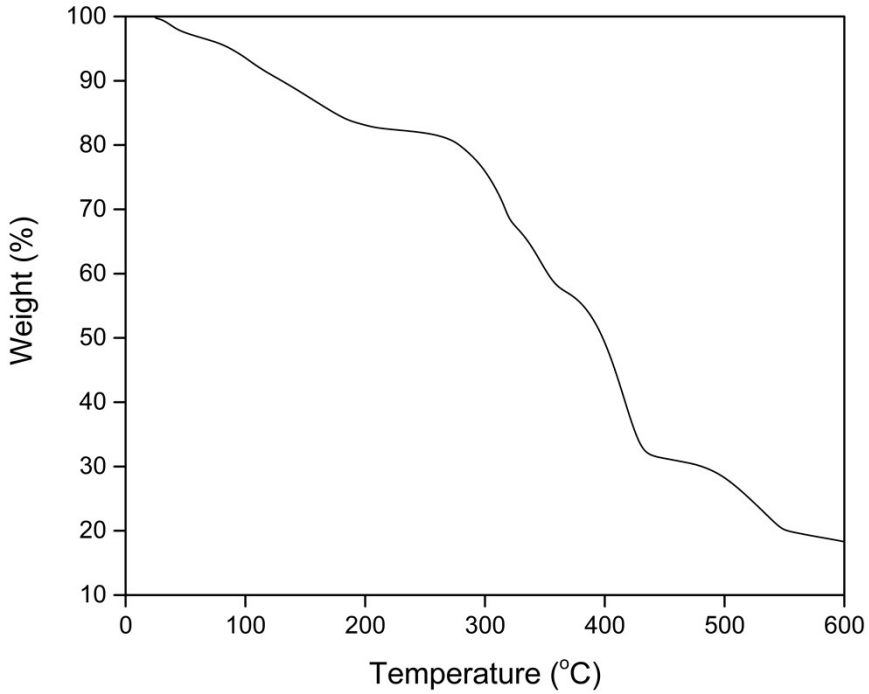

Figure S2. Thermal gravimetric analysis of **CdTzTz** from 25-600 °C at 2 °C min^{-1}.

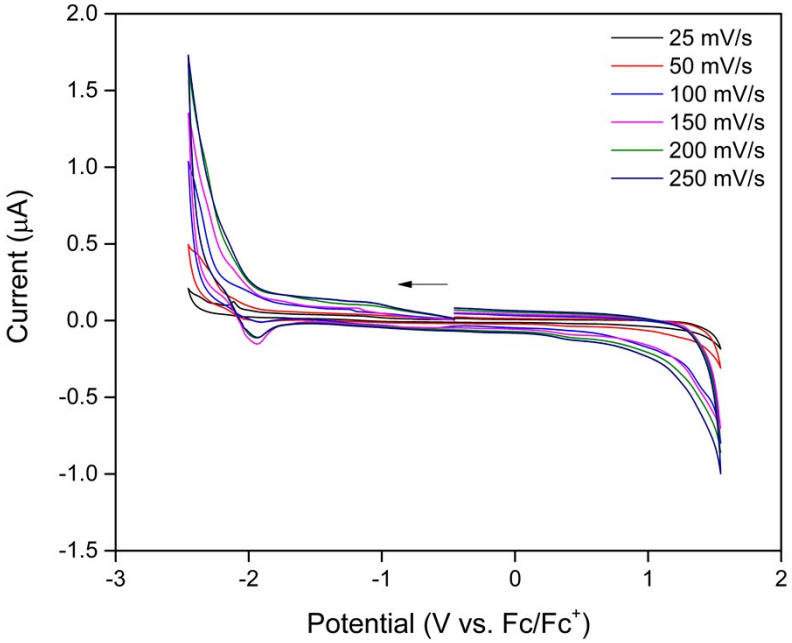

Figure S3. Solid-state cyclic voltammogram of **CdTzTz** in 0.1 M $[(n\text{-}C_4H_9)_4N]PF_6$/MeCN electrolyte at scan rates of 25-250 mV s^{-1}. The arrow indicates the direction of the forward scan.

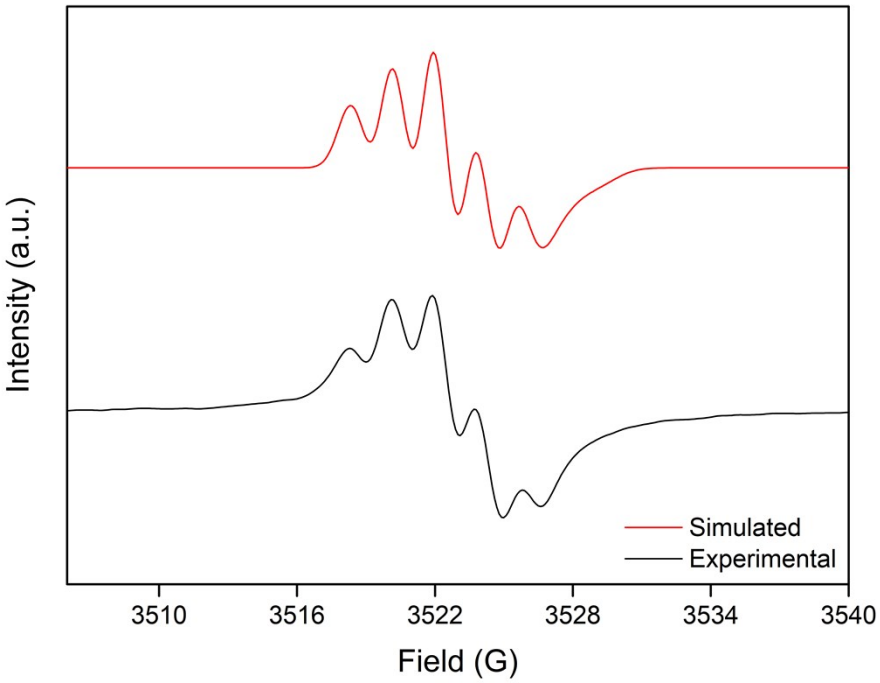

Figure S4. Experimental *vs*. simulated spectra of the BPPTzTz EPR signal at -2.0 V using a simulated *g*-value of 2.0041 and ^{14}N hyperfine coupling constants of 5.2 MHz (0.18 mT) and 4.8 MHz (0.17 mT).

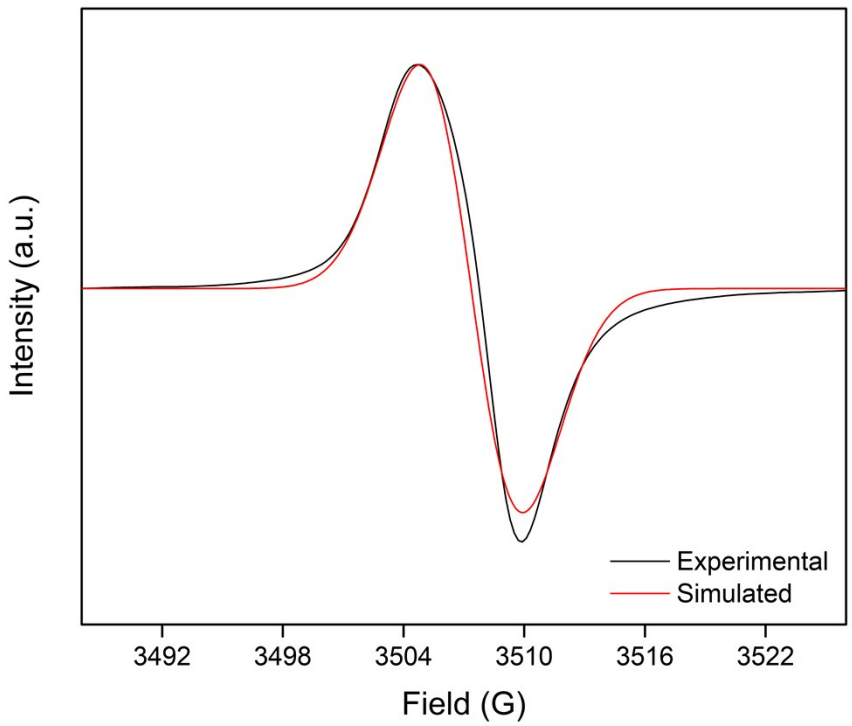

Figure S5. Experimental *vs*. simulated spectra of the **CdTzTz** EPR signal at -2.0 V using an isotropic model with a simulated *g*-value of 2.0147.

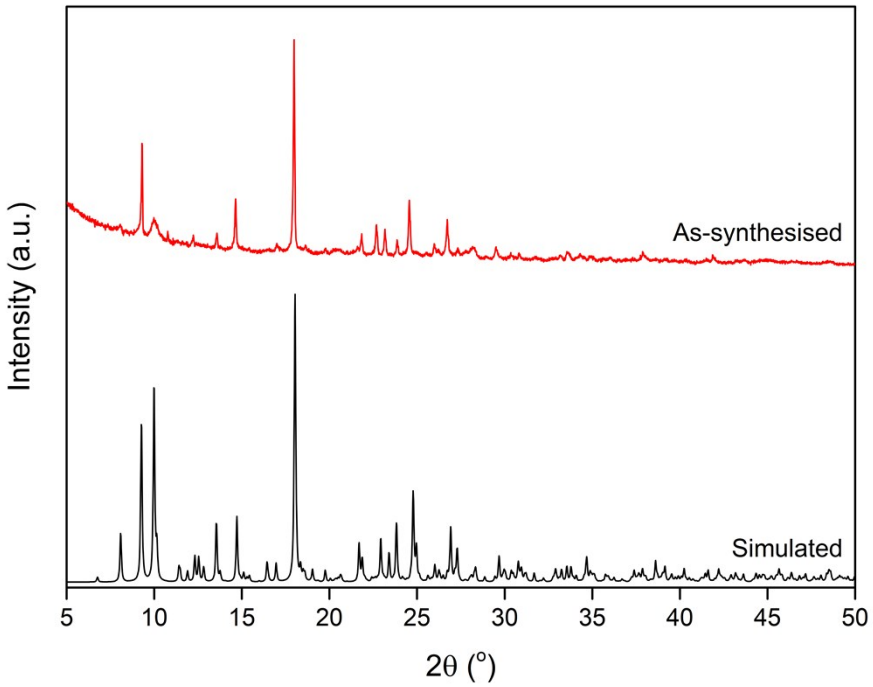

Figure S6. PXRD of **CdTzTz** showing the simulated and as-synthesised patterns to demonstrate phase purity of the bulk **CdTzTz** material.

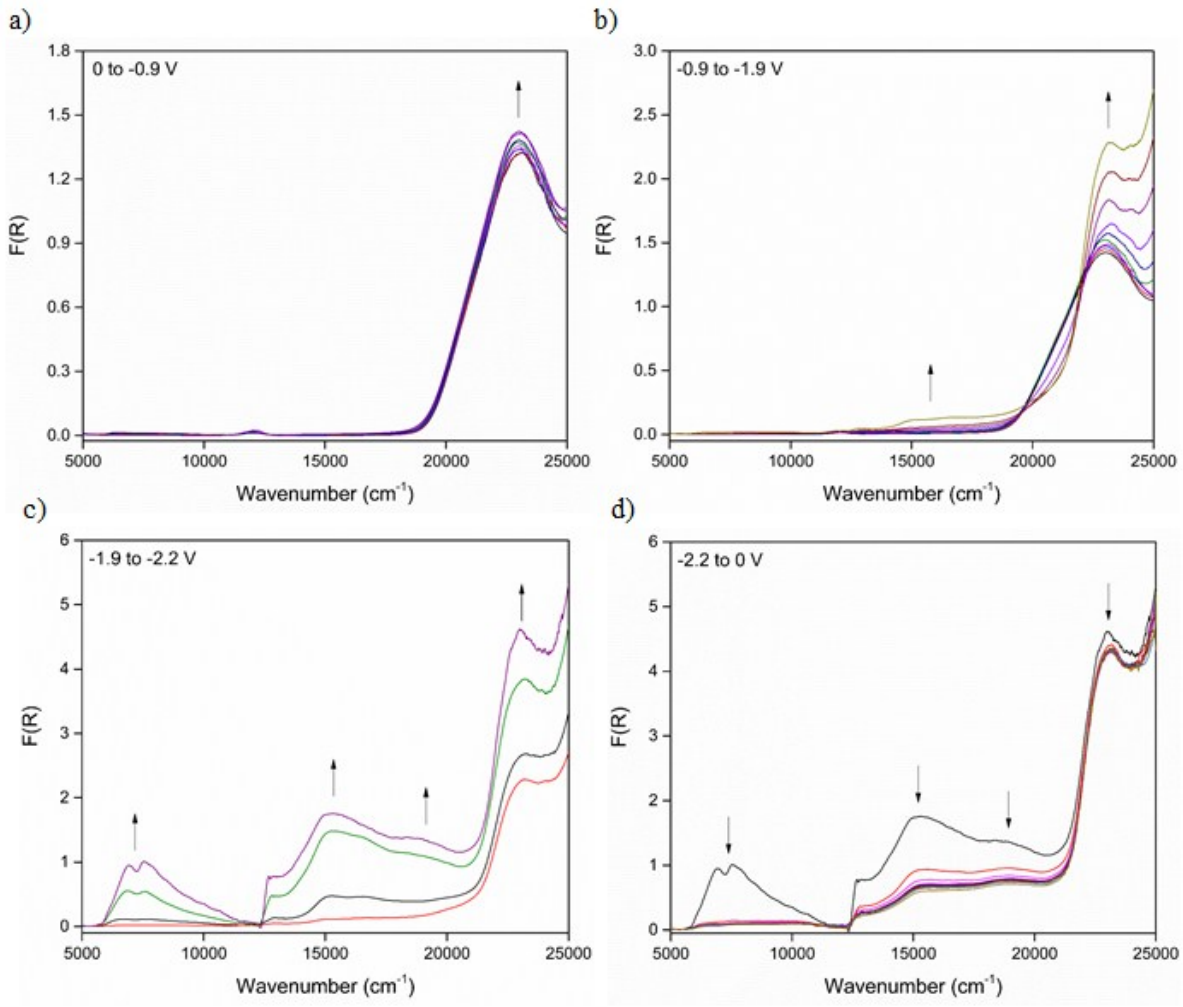

Figure S7. Solid-state UV-Vis-NIR spectroelectrochemistry of **CdTzTz** showing in 0.1 M $[(n\text{-}C_4H_9)_4N]PF_6$/MeCN electrolyte showing potential decreases from a) 0 to -0.9 V, b) -0.9 to -1.9 V, c) -1.9 to -2.2 V and d) -2.2 to 0 V, where the arrows indicate the direction of the spectral progression. The step at 12500 cm^{-1} is due to the detector change.

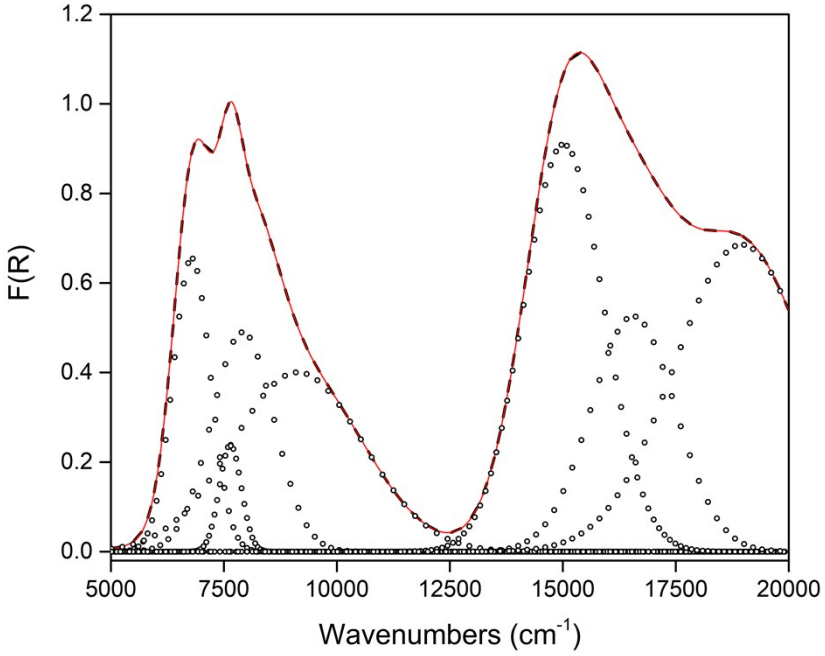

Figure S8. Experimental spectrum (black dashed) vs. deconvoluted curvefit (red) of the solid-state UV-Vis-NIR spectrum of the mixed-valence form of **CdTzTz** with underlying Gaussian components (dotted) of the deconvolution. Gaussian deconvolution was performed using the GRAMS suite of software.

Equations Used to Derive Charge Transfer Parameters

Theoretical bandwidth:

$$\Delta\nu_{1/2}{}^{o} = [2310(\nu_{max})]^{1/2} \quad \text{(Eqn. 1)}$$

where ν_{max} is the position of the relevant band (in cm^{-1}).[8,9] Note that the "theoretical" bandwidth here is a semi-empirical quantity derived from the position of the band maximum ν_{max}.

Tunnelling matrix element:

$$T_{da} = [(4.2 \times 10^{-4}) \times \varepsilon_{max}\Delta\nu_{1/2}E_{op}]^{1/2}/d \quad \text{(Eqn. 2)}$$

where E_{op} is the energy of the IVCT band (ν_{max} in cm^{-1}), ε_{max} is the extinction coefficient (in M^{-1} cm^{-1}) and d is the charge transfer distance (equivalent to r_{ab} from Eqn. 7, in Å). All quantities in cm^{-1} are divided by 10^3 as per this equation's definition by Hush.[9,10]

Frequency factor:

$$\nu_{et} = [4\pi^2 T_{da}{}^2 / h](\pi / k_B T\lambda)^{1/2} \quad \text{(Eqn. 3)}$$

where h is Planck's constant (4.136×10^{-15} eV s), k_B is Boltzmann's constant (8.617×10^{-5} eV K^{-1}), T is the temperature (300 K) and λ (i.e. ν_{max}) is the energy of the IVCT band (in eV).[11]

Mobility:

$$k = \nu_{et}\, e^{\frac{-\chi}{4RT}} \quad \text{(Eqn. 4)}$$

where χ is the molar energy of electron transfer obtained by multiplying λ (i.e. ν_{max}) with Avogadro's constant and R is the ideal gas constant ($8.314 \times 6.242 \times 10^{18}$ eV K^{-1} mol^{-1}).[11]

Quantification of the IVCT Bands *via* Single Crystal UV-Vis Absorption Spectroscopy

The traditional method of quantifying mixed valency and IVCT from spectroscopic data relies on the application of Marcus-Hush theory. This approach is problematic in MOFs and other solid-state systems due to the requirement of a molar extinction coefficient for the system under study. Such an extinction coefficient can be calculated from the application of the Beer-Lambert law (Eqn. 5) using the absorbance of the relevant band and concentration of the analyte, parameters which are readily obtained in solution-state systems. As UV-Vis-NIR data of solid-state systems is typically obtained as diffuse reflectance, an absorbance value and concentration cannot be readily obtained. In order to quantify the IVCT bands of the mixed-valence **CdTzTz** material, a single crystal UV-Vis experiment using the method of Krausz,[12] was performed on a single crystal of the neutral **CdTzTz** and **ZnTzTz** materials to obtain the solid-state absorption spectrum (Figure S6). Care was taken to choose a well-defined single crystal, i.e. with a regular morphology and no cracks or satellite crystallites, to prevent undesirable absorption or scattering effects.

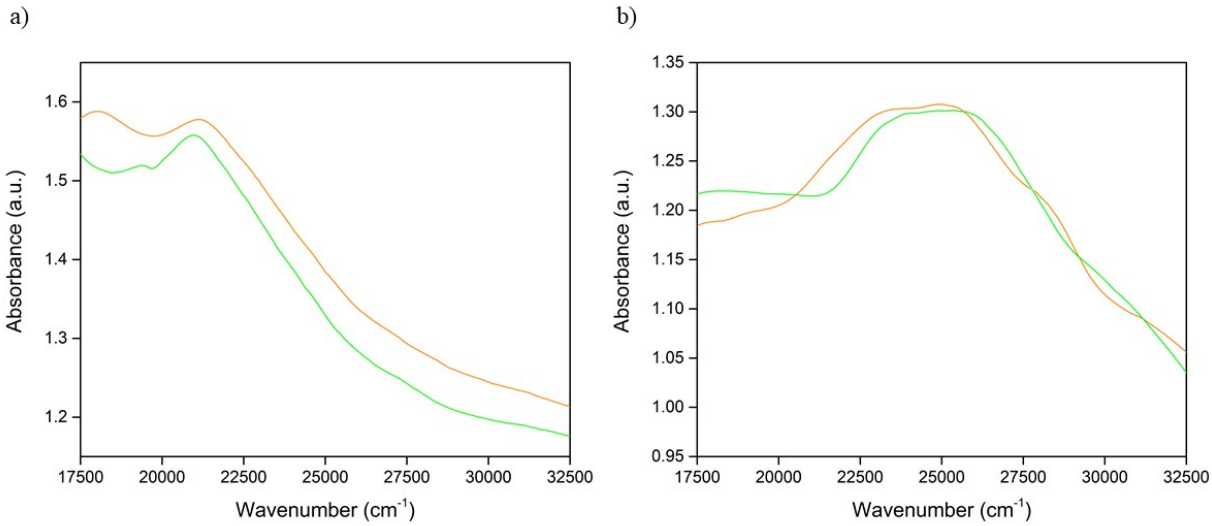

Figure S9. Single crystal UV-Vis spectra of a) **CdTzTz** and b) **ZnTzTz** showing absorbance in both parallel (orange) and perpendicular (green) polarisation modes. The two modes are relative to the plane of polarisation of the incident light.

Such an absorption spectrum can be analysed using the Beer-Lambert law.

$$A = \varepsilon c l \qquad \text{(Eqn. 5)}$$

The value of the absorbance pathlength (l) was obtained from measurement of the physical dimensions of the crystal using the optical viewer of a single crystal X-ray diffractometer.

Although beyond the scope of this study, polarisation effects arising from orientation of the chromophores in the solid-state structure can be studied by indexing the crystal faces and mounting the crystal on the spectrometer along the axis of interest.

The solid-state molar extinction coefficient was derived from the number concentration definition:

$$n = \frac{n}{\overline{V}} = \frac{N}{N_A V} \qquad \text{(Eqn. 6)}$$

where N is the number of chromophores per crystallographic unit cell, N_A is Avogadro's constant and V is the unit cell volume (Å^3). Using the **CdTzTz** structure as an example, the number of BPPTzTz chromophores in the asymmetric unit is one, hence N is equal to the Z number of the structure to give 8 BPPTzTz chromophores per unit cell. Evaluating Eqn. 6 with these parameters yielded a solid-state molar concentration value of 1.72 M for the **CdTzTz** and 1.78 M for the **ZnTzTz** materials respectively. The solid-state molar extinction coefficient of both materials was then derived from the Beer-Lambert law (Table S3).

Table S3. Spectral parameters derived from single crystal UV-Vis spectroscopy of **CdTzTz** and **ZnTzTz**.

Parameter	ZnTzTz	CdTzTz
N	8	8
Concentration (M)	1.78	1.72
Pathlength (cm)	0.0072	0.0041
Absorbance Maximum (a.u.)	1.31	1.56
Molar Extinction Coefficient (M^{-1} cm^{-1})	102	221

Given that the molar extinction coefficients had been calculated for the neutral MOFs, the extinction coefficient of the mixed-valence species could be calculated by multiplying this by the ratio of the neutral and NIR band F(R) values. An assumption to note here is that the extinction coefficient values are linear across the entire wavelength range. From these, the electronic coupling constants (H_{ab}) of the NIR IVCT bands of both materials could be calculated by applying the Marcus-Hush equation (Eqn. 7).[8,9]

$$H_{ab} = [0.0205 \times (\nu_{max}\varepsilon\Delta\nu_{1/2})^{1/2}] / r_{ab} \qquad \text{(Eqn. 7)}$$

where ν_{max} is the energy of the IVCT band and $\Delta\nu_{1/2}$ is the bandwidth obtained from deconvolution, ε is the extinction coefficient of the IVCT band and r_{ab} is the crystallographically determined distance between the cofacial BPPTzTz ligand pair (in Å). Evaluating this equation with the derived parameters obtained from deconvolution of the diffuse reflectance spectra yielded the H_{ab} of the mixed-valence **CdTzTz** and **ZnTzTz** MOFs (Table S4 and S5).

Table S4. Spectral data of the deconvoluted diffuse reflectance spectrum and associated parameters used to derive the H_{ab} values for the mixed-valence form of **ZnTzTz**.[1]

ν_{max} (cm^{-1})*	F(R)$_{max}$ (a.u.)	$\Delta\nu_{1/2}$ (cm^{-1})	$\Delta\nu_{1/2}^{o}$ (cm^{-1})	ε (M^{-1} cm^{-1})	H_{ab} (cm^{-1})
6576	2.08	1465	3898	37.3	103
8202	4.82	2939	4353	86.4	247
10773	1.78	2757	2524		
13409	1.69	2856	2569		
15310	6.61	2104	2205		
16685	1.40	1188	1657		
17583	7.16	2531	2418		

* Note that the cofacial stacking distance of **ZnTzTz** was previously quoted as 3.80 Å having been calculated as the average of the S···S distances on TzTz cores which has now, for the purposes of comparison with **CdTzTz**, been redefined as 3.782(8) Å from the centroid-to-centroid distance defined using the atoms of the TzTz moiety.

Table S5. Spectral data of the deconvoluted diffuse reflectance spectrum and associated parameters used to derive the H_{ab} values for the mixed-valence form of **CdTzTz**.

ν_{max} (cm^{-1})	F(R)$_{max}$ (a.u.)	$\Delta\nu_{1/2}$ (cm^{-1})	$\Delta\nu_{1/2}^{o}$ (cm^{-1})	ε (M^{-1} cm^{-1})	H_{ab} (cm^{-1})
6786	0.655	976	3959	108.8	145
7642	0.239	570	4202	39.7	71
7916	0.490	1620	4276	81.4	175
9134	0.401	3402	4593	66.6	246
15016	0.910	2084	5890		
16556	0.526	2209	6184		
18956	0.686	3514	6617		

Due to the substantial intramolecular character of the NIR transitions (see Figure 4 (a) of the main text), the H_{ab} value calculated for the 9134 cm^{-1} transition of 246 cm^{-1} serves as an upper limit for the strength of the electronic coupling.

References

1. Hua, C.; Doheny, P. W.; Ding, B.; Chan, B.; Yu, M.; Kepert, C. J.; D'Alessandro, D. M. *J. Am. Chem. Soc.* **2018**, *140*, 6622-6630.
2. Aragao, D.; Aishima, J.; Cherukuvada, H.; Clarken, R.; Clift, M.; Cowieson, N. P.; Ericsson, D. J.; Gee, C. L.; Macedo, S.; Mudie, N.; Panjikar, S.; Price, J. R.; Riboldi-Tunnicliffe, A.; Rostan, R.; Williamson, R.; Caradoc-Davies, T. T. *J. Synchrotron Rad.* **2018**, *25*, 885-891.
3. Sheldrick, G. *Acta Cryst.* **2015**, *A71*, 3-8.
4. Sheldrick, G. *Acta Cryst.* **2015**, *C71*, 3-8.
5. Hubschle, C. B.; Sheldrick, G. M.; Dittrich, B. *J. App. Cryst.* **2011**, *44*, 1281-1284.
6. Spek, A. *Acta Cryst.* **2009**, *D65*, 148-155.
7. Bruker Bruker AXS Inc., Madison, Wisconsin, USA, 2001.
8. Allen, G. C.; Hush, N. S. *Prog. Inorg. Chem.* **1967**, *8*, 357-390
9. Hush, N. S. *Prog. Inorg. Chem.* **1967**, *8*, 391-444.
10. Hush, N. S. *Electrochim. Acta* **1968**, *13*, 1005-1023.
11. Meyer, T. J. *Chem. Phys. Lett.* **1979**, *64*, 417-420.

12. Krausz, E. *Aust. J. Chem.* **1993**, *46*, 1041-1054.